

7 Vehicle dynamics in the asymmetry plane

7.1 Equations of motion of a simple vehicle model

Consider a simple consisting of a rear wheel and a steerable front wheel movable in the plane. This is the simplest model which can be formulated which gives essential information about the dynamics of a vehicle, known as the one-track or bicycle model.

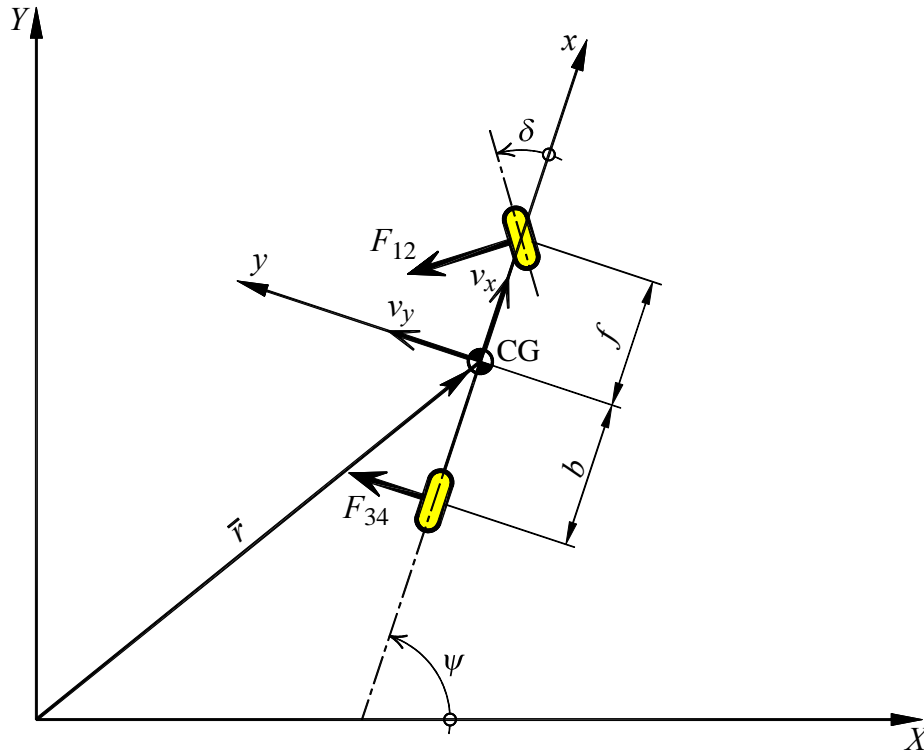


Figure 7.1-1 The one-track or bicycle model.

Note that the two wheels per axle has been substituted by a single one. In practice, this means that the height over ground of the centre of gravity is assumed to be zero.

A body fixed coordinate system (CG, x, y, z) is attached to the centre of gravity of the vehicle. Additionally, an inertial coordinate system (O, X, Y, Z) is defined.

The velocity vector for the centre of gravity, CG, is expressed as

$$\dot{\vec{r}} = v_x \hat{x} + v_y \hat{y} \quad (7.1.1)$$

and the vehicle's yaw velocity $\bar{\omega} = \dot{\psi} \hat{z}$

where $\dot{\psi} = \frac{d\psi}{dt}$

Differentiation rules

At several occasions, the following differentiation rules for vectors will be used:

$$\frac{d\bar{f}}{dt} = \frac{\partial \bar{f}}{\partial t} + \bar{\omega} \times \bar{f}$$

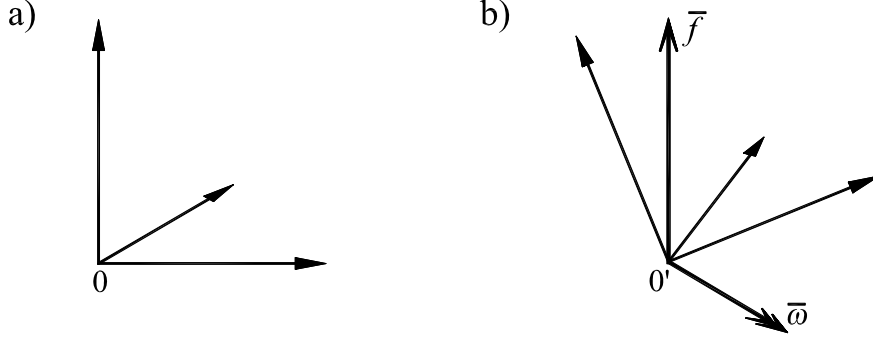


Figure 7.1-2 Two coordinate systems.

Assume that the (0')-system rotates with the rotational vector $\bar{\omega}$ relative to the inertial system (0).

$\frac{\partial \bar{f}}{\partial t}$ is the derivative with respect to t in the (0')-system.

If \bar{f} is a *fixed* vector in the (0')-system, then $\frac{d\bar{f}}{dt} = \bar{\omega} \times \bar{f}$.

Based on the vehicle model in figure 7.1-1 and the differentiation rule above, the velocities for the midpoints of the front- and rear axles can be expressed as:

$$\dot{\bar{r}}_f = \dot{\bar{r}} + \bar{\omega} \times (f, 0, 0) = v_x \hat{x} + (v_y + \dot{\psi} f) \hat{y} \quad (7.1.2)$$

$$\dot{\bar{r}}_b = \dot{\bar{r}} + \bar{\omega} \times (-b, 0, 0) = v_x \hat{x} + (v_y - \dot{\psi} b) \hat{y} \quad (7.1.3)$$

and thereby the slip angles

$$\alpha_{12} = \arctan\left(\frac{v_y + \dot{\psi} f}{v_x}\right) - \delta \quad (7.1.4)$$

$$\alpha_{34} = \arctan\left(\frac{v_y - \dot{\psi} b}{v_x}\right) \quad (7.1.5)$$

for the front- and rear wheels, respectively.

By differentiation of the velocity vector, the acceleration of the centre of gravity is obtained, expressed in the body fixed coordinate system (CG, x, y, z)

$$\ddot{\vec{r}} = \dot{v}_x \hat{x} + \dot{v}_y \hat{y} + \bar{\omega} \times (v_x \hat{x} + v_y \hat{y}, 0) = (\dot{v}_x - \dot{\psi} v_y) \hat{x} + (\dot{v}_y + \dot{\psi} v_x) \hat{y} \quad (7.1.6)$$

Assume that the only external forces that affect the motion of the vehicle in the plane are the tyre forces. The side forces are in this simple model assumed to be linear functions of the slip angles:

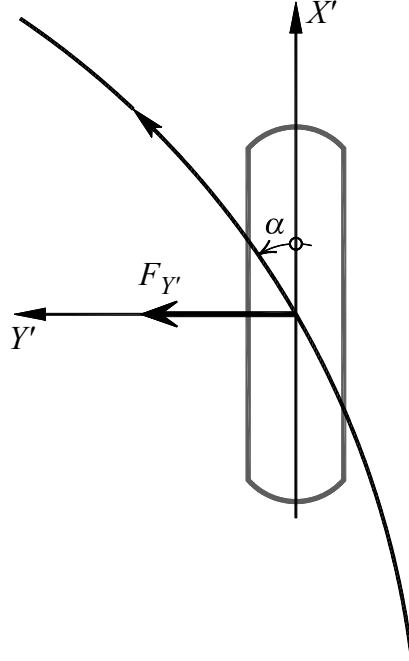


Figure 7.1-3 Slip angle and side force for a tyre.

$$F_{12} = -C_{12} \alpha_{12}$$

$$F_{34} = -C_{34} \alpha_{34}$$

where C_{12} and C_{34} are the cornering stiffnesses for the front and rear axle respectively. Denoting the mass of the vehicle m , and the inertia around the z -axis through the centre of gravity J_z , the equations of motion become:

$$\uparrow m(\dot{v}_x - \dot{\psi} v_y) = -F_{12} \sin \delta$$

$$\rightarrow m(\dot{v}_y + \dot{\psi} v_x) = F_{34} + F_{12} \cos \delta$$

$$J_z \ddot{\psi} = f F_{12} \cos \delta - b F_{34}$$

To analyze the yaw motion and stability, make the assumptions

1. $\alpha_{12}, \alpha_{34}, \delta \ll 1$
2. constant speed v_x

This simplifies the equations of motion to

$$m(Dv_y + \dot{\psi} v_x) = -C_{34} \frac{v_y - \dot{\psi} b}{v_x} - C_{12} \left(\frac{v_y + \dot{\psi} f}{v_x} - \delta \right)$$

$$J_z D \dot{\psi} = -f C_{12} \left(\frac{v_y + \dot{\psi} f}{v_x} - \delta \right) + b C_{34} \frac{v_y - \dot{\psi} b}{v_x}$$

and in matrix form

$$\begin{pmatrix} mD + \frac{C_{12} + C_{34}}{v_x} & mv_x + \frac{f C_{12} - b C_{34}}{v_x} \\ \frac{f C_{12} - b C_{34}}{v_x} & J_z D + \frac{f^2 C_{12} + b^2 C_{34}}{v_x} \end{pmatrix} \begin{pmatrix} v_y \\ \dot{\psi} \end{pmatrix} = \begin{pmatrix} C_{12} \\ f C_{12} \end{pmatrix} \delta \quad (7.1.7)$$

Introducing the system matrix A , equation 7.1.7 can be compactly expressed as:

$$A \begin{pmatrix} v_y \\ \dot{\psi} \end{pmatrix} = \begin{pmatrix} C_{12} \\ f C_{12} \end{pmatrix} \delta \quad (7.1.8)$$

7.2 Stationary driving

First, consider the simple stationary case, $D = 0$, i.e. $\dot{v}_y = \ddot{\psi} = 0$. From the resulting system of algebraic equations, solve for $\dot{\psi}$ and v_y as functions of δ .

For example, use Cramer's rule which needs a value for $\det A$:

$$\det A = \frac{(C_{12} + C_{34})(f^2 C_{12} + b^2 C_{34}) - (f C_{12} - b C_{34})^2}{v_x^2} - m(f C_{12} - b C_{34}) =$$

$$= \frac{L^2}{v_x^2} C_{12} C_{34} + m(b C_{34} - f C_{12})$$

where the wheel base $L = f + b$

It follows that:

$$\frac{v_y}{\delta} = \frac{\begin{vmatrix} C_{12} & mv_x + \frac{f C_{12} - b C_{34}}{v_x} \\ f C_{12} & \frac{f^2 C_{12} + b^2 C_{34}}{v_x} \end{vmatrix}}{\det A} =$$

$$(7.2.1)$$

$$= \frac{v_x (b \cdot L \cdot C_{12} C_{34} - f C_{12} \cdot m v_x^2)}{L^2 C_{12} C_{34} + m \cdot v_x^2 (b C_{34} - f C_{12})}$$

And similarly that
$$\frac{\dot{\psi}}{\delta} = \frac{v_x \cdot L C_{12} \cdot C_{34}}{L^2 C_{12} \cdot C_{34} + m v_x^2 (b C_{34} - f C_{12})} \quad (7.2.2)$$

Some interesting conclusions can be drawn. Both expressions contain a denominator which can go to zero under certain circumstances. Assume that

$$B = b C_{34} - f C_{12} < 0$$

Then the denominator goes to zero when

$$v_x \rightarrow v_{krit} = \sqrt{\frac{L^2 C_{12} C_{34}}{m(f C_{12} - b C_{34})}} \quad (7.2.3)$$

i.e. both $\frac{v_y}{\delta}$ and $\frac{\dot{\psi}}{\delta}$ grow without bound. The sign of B obviously have a fundamental significance for the steering response of the vehicle.

7.3 Stationary circular driving

For a vehicle with the speed v_x which is driven in a large circle (such that $v_y \ll v_x$) with the radius R , it follows that

$$R \cdot \dot{\psi} = v_x \quad (7.3.1)$$

and the lateral acceleration

$$a_y = \frac{v_x^2}{R} = v_x \cdot \dot{\psi} \quad (7.3.2)$$

Equation (7.3.1) and (7.3.2) substituted into (7.2.2) gives

$$\delta = \frac{L}{R} + \frac{m v_x^2 (b C_{34} - f C_{12})}{R \cdot L C_{12} \cdot C_{34}} \quad (7.3.3)$$

The relation between v_x and δ thus looks like in figure 7.3-1.

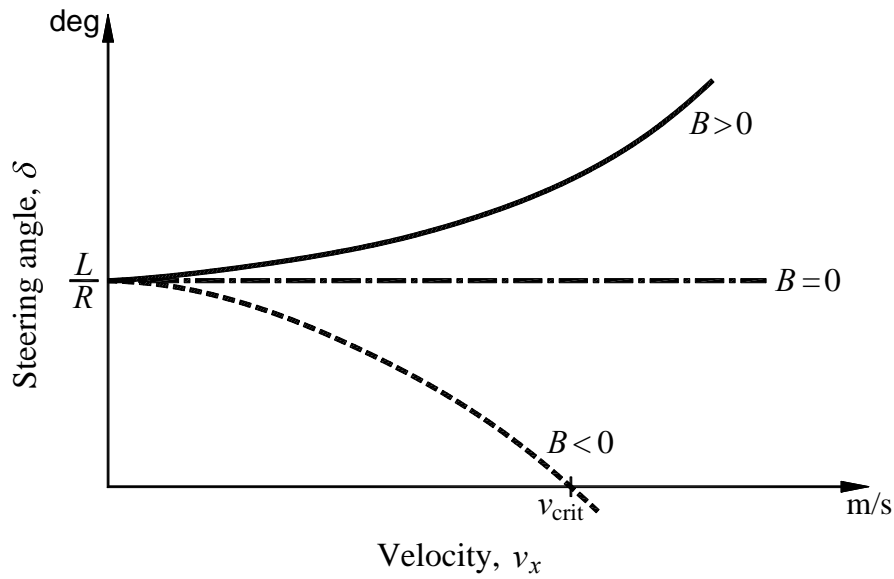


Figure 7.3-1 Steering response for different signs of the factor B .

If $B = b C_{34} - f C_{12} = 0$ then

$$\delta = \frac{L}{R} \quad (7.3.4)$$

for all v_x . The vehicle is then said to be *neutral steer*. This means that the steering wheel angle is constant for different velocities, when driving in a circle with fixed radius R .

If $B < 0$, an increasing speed v_x means a smaller steering wheel angle is needed to keep the vehicle on the same circular path. Eventually, negative steering wheel angles are needed to remain on the circular path. A vehicle with this characteristic is usually called *oversteer*. It is interesting to note that the steering angle $\delta = 0$ is needed for the speed

$$v_x = \sqrt{\frac{C_{12} C_{34} L^2}{m(f C_{12} - b C_{34})}}$$

i.e. the critical speed.

If $B > 0$, on the other hand, larger steering wheel angles are needed for increasing speed. The vehicle tends to move straight forward instead of following the steering wheel angle, and the vehicle is called *understeer*.

Furthermore, from equation (7.3.3) it follows that the steering angle $\delta = L/R$ is the steering angle which is needed to keep the turning radius R at very low speeds, *independently* of whether the vehicle is over- or understeer. This angle is sometimes called the *Ackermann-angle*, δ_A , which is defined as

$$\delta_A = \frac{L}{R} \quad (7.3.5)$$

and corresponds to the geometrical steering angle described in figure 7.3-2.

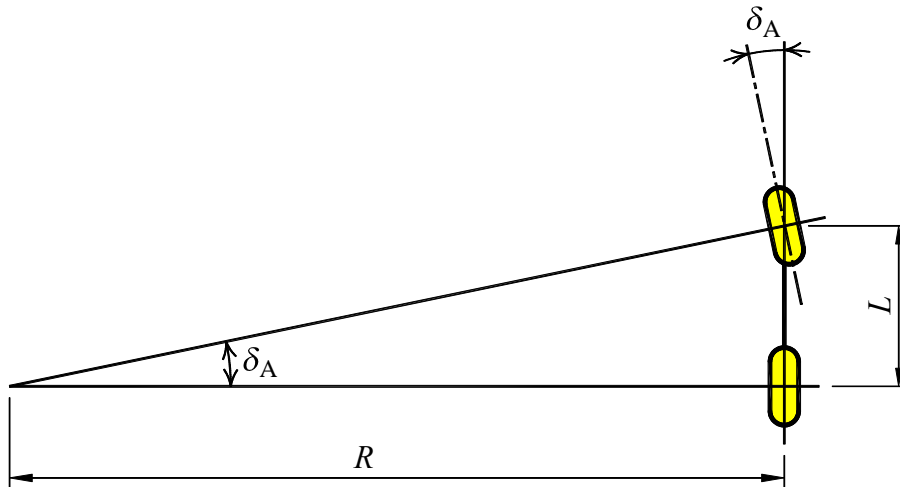


Figure 7.3-2 Ackermann-angle.

From equations (7.3.2), (7.3.3) and (7.3.5) it also follows that

$$\delta = \delta_A + K_{us} \cdot a_y \quad (7.3.6)$$

where

$$K_{us} = \frac{m \cdot (b C_{34} - f C_{12})}{L \cdot C_{12} \cdot C_{34}} \quad (7.3.7)$$

only depends on vehicle properties and is usually called the *understeer gradient*.

7.4 Definition of understeer

In the previous section it was shown that the steering response of a vehicle is dependent on the cornering stiffnesses C_{12} , C_{34} and the position of the centre of gravity. For practical use it has, however, been desirable to have a definition which is based on measurable quantities which are easily sensed by the driver at the steering wheel. The consensus has been that the applied steering wheel angle and the lateral acceleration are two such significant quantities, and the following definition of the *understeer gradient*, K_{us} , has been internationally agreed upon:

$$K_{us} = \frac{1}{i_s} \frac{\partial \delta_{SW}}{\partial a_y} - \frac{\partial \delta_A}{\partial a_y} \quad (7.4.1)$$

where: i_s = steering ratio between steering wheel and front wheel angle

δ_{SW} = angle of steering wheel

a_y = lateral acceleration

δ_A = Ackermann-angle

$\frac{\partial f}{\partial x}$ = quotient between the change of f and the change of x from a given equilibrium state

This definition contains a couple of new concepts. The steering angle of the wheels are connected to the angle of the steering wheel by

$$\delta_{SW} = i_s \cdot \delta$$

which implies

$$\frac{1}{i_s} \frac{\partial \delta_{SW}}{\partial a_y} = \frac{\partial \delta}{\partial a_y}$$

and partial differentiation of equation (7.3.6) with respect to a_y gives agreement between equations (7.3.7) and (7.4.1).

The understeer gradient can also be expressed via the front and rear slip angles. As noted earlier, the force and torque equilibrium equations are

$$\begin{cases} F_{12} + F_{34} = m \cdot a_y \\ f F_{12} - b F_{34} = 0 \end{cases}$$

With linear tyres the equations can be expressed as:

$$\begin{cases} -C_{12} \alpha_{12} - C_{34} \alpha_{34} = m a_y \\ f C_{12} \alpha_{12} = b C_{34} \alpha_{34} \end{cases}$$

which implies the slip angles

$$\alpha_{12} = -\frac{m \cdot b}{L C_{12}} \cdot a_y$$

$$\alpha_{34} = -\frac{m \cdot f}{L C_{34}} \cdot a_y$$

$$\alpha_{12} - \alpha_{34} = -\frac{m}{L} \frac{b C_{34} - f C_{12}}{C_{12} C_{34}} a_y = -K_{us} \cdot a_y \quad (7.4.2)$$

The difference between the slip angles front and rear are thus proportional to the lateral acceleration with the understeer gradient as a proportionality factor.

7.5 Circular driving tests

There are in principle two ways of performing circular driving tests. Either a *constant turning radius* is chosen and the steering angle is adapted to the desired speed, or a *constant speed* is chosen and the steering angle is adapted to the desired lateral acceleration

Use equations (7.3.6), (7.3.5) and (7.3.2):

$$\delta = \delta_A + K_{us} \cdot a_y$$

$$a_y = \frac{v_x^2}{R}$$

$$\delta_A = \frac{L}{R}$$

7.5.1 Circular driving test with constant radius

R is here constant. This case is previously described in section 7.3:

$$\delta = \frac{L}{R} + K_{us} \cdot a_y$$

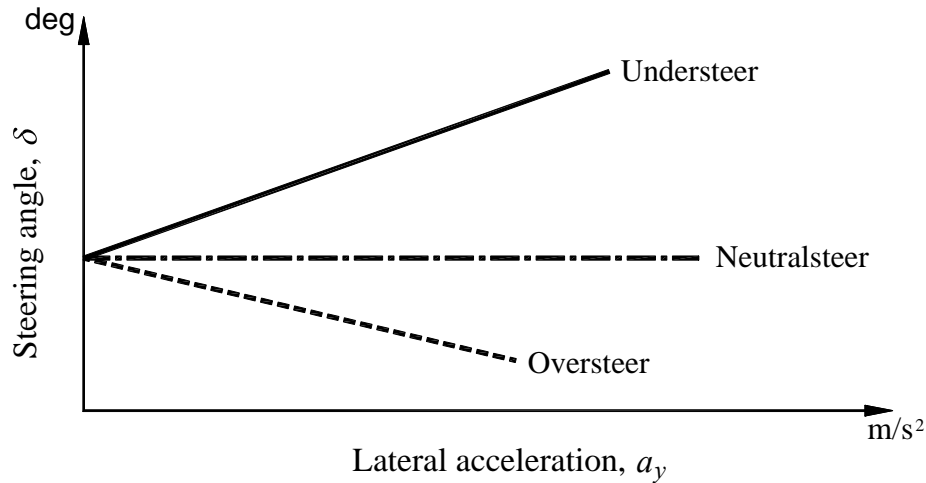


Figure 7.5-1 Circular driving tests with hypothetical, perfectly linear vehicles.

The understeer gradient is the slope of the respective curve in figure 7.5-1. In reality, the lines will not be perfectly linear as in this case. K_{us} is then instead given by the slope of the tangent at each point.

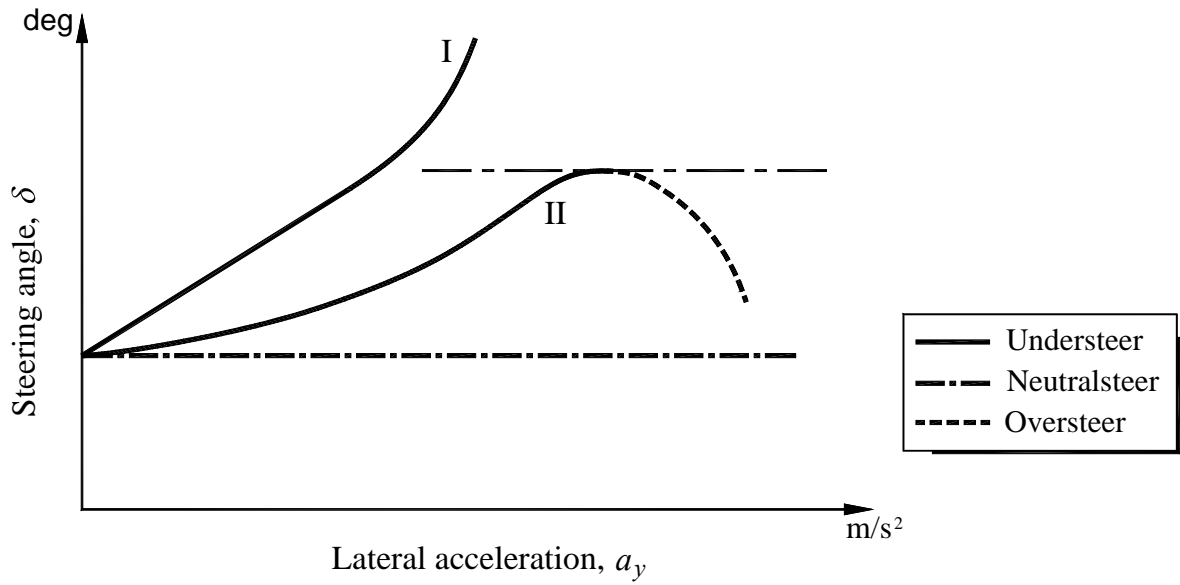


Figure 7.5-2 Circular driving tests with example nonlinear vehicles.

Vehicle I, in figure 7.5-2, understeer in the whole range, whereas vehicle II understeer for low accelerations, and oversteer for high accelerations.

7.5.2 Circular driving with constant speed

The speed v_x is here constant. Then it follows that

$$\delta_A = \frac{L}{R} = \frac{L}{v_x^2} \cdot a_y \quad \text{and} \quad \delta = \left(\frac{L}{v_x^2} + K_{us} \right) \cdot a_y$$

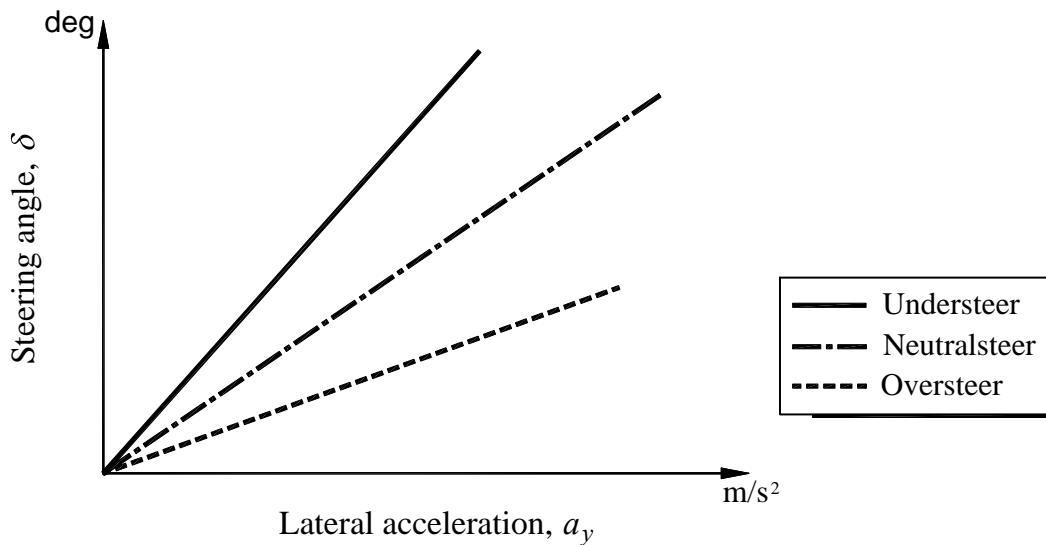


Figure 7.5-3 Circular driving test with constant speed; hypothetical, perfectly linear vehicles.

In analogy with the previous case, the measurement results of a circular driving test will be nonlinear for real vehicles, see figure 7.5-4.

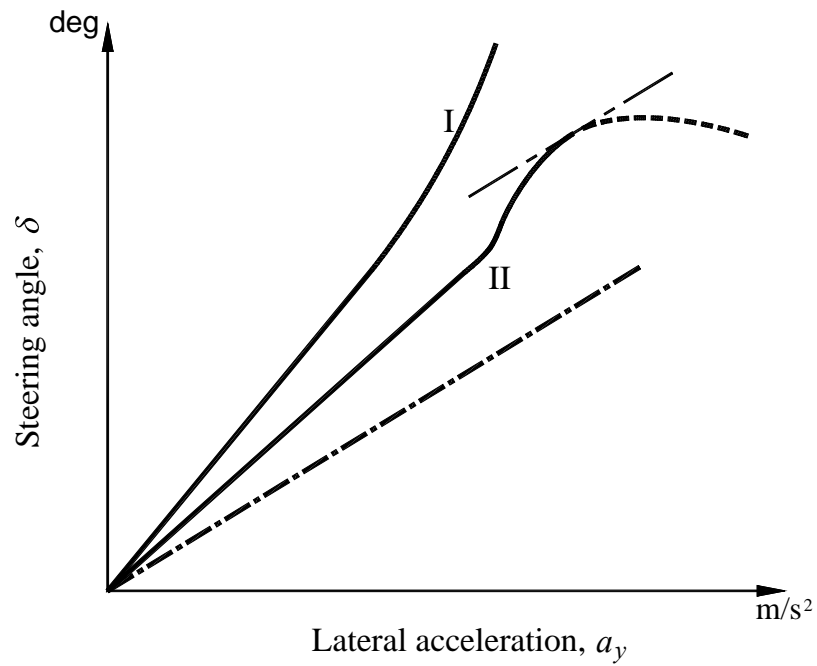


Figure 7.5-4 Circular driving tests with example nonlinear vehicles.

Vehicle I and II in figure 7.5-4 are the same as in figure 7.5-2 in the previous section.

7.6 Steering sensitivity

In the previous sections the steering angles necessary for a given vehicle in a steady state cornering manoeuvre has been investigated. It could also be of interest to study the steering sensitivity under these conditions, i.e. the quotient between for example the angular velocity and the steering wheel angle. Equation (7.2.2) is precisely the expression for this quantity in the stationary case:

$$\frac{\dot{\psi}}{\delta} = \frac{v_x \cdot L \cdot C_{12} \cdot C_{34}}{L^2 C_{12} C_{34} + m \cdot v_x^2 (b C_{34} - f C_{12})} = \frac{v_x}{L + K_{us} v_x^2} \quad (7.6.1)$$

Depending on the sign of K_{us} , there are three different cases.

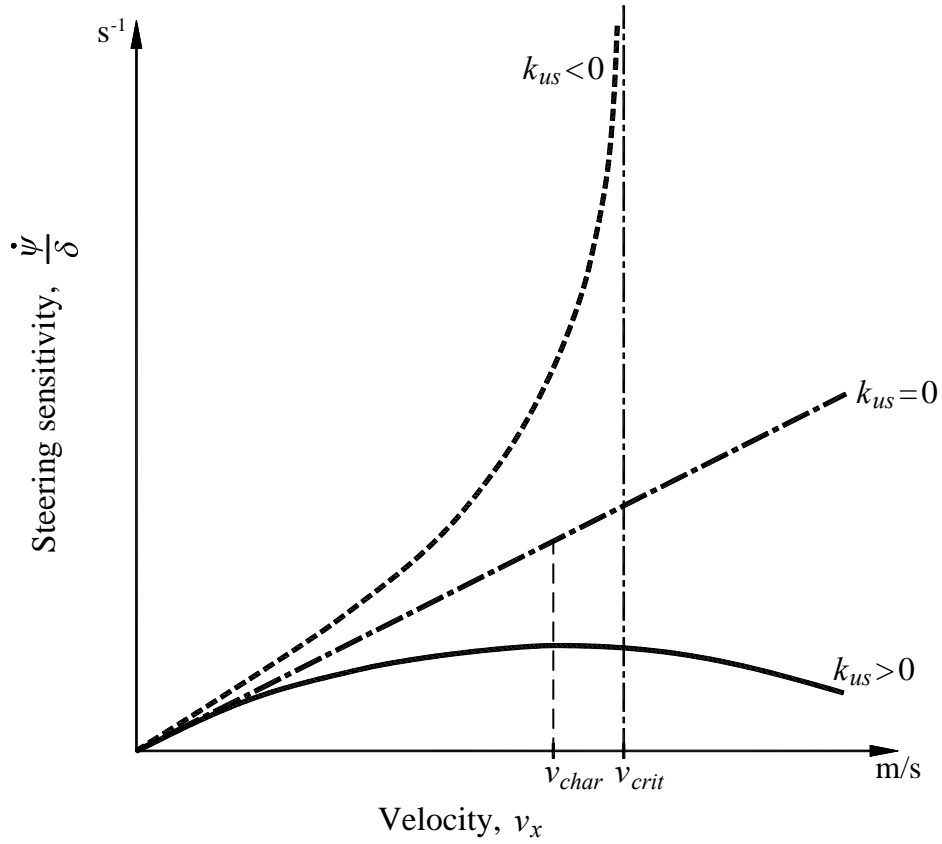


Figure 7.6-1 Steering sensitivity for different signs of the understeer gradient.

I If $K_{us} < 0$ the steering sensitivity has a vertical asymptote for

$$L + K_{us} v_x^2 = 0$$

i.e.
$$v_x = \sqrt{\frac{L}{-K_{us}}} = \sqrt{\frac{C_{12} C_{34} L^2}{m(f C_{12} - b C_{34})}} = v_{krit}$$

which according to equation (7.2.3) coincides with the *critical speed*, v_{krit} . This concerns the oversteer vehicle, and is therefore only of theoretical interest since all vehicles are designed more or less understeer.

II The neutral steer vehicle with $K = 0$ has a steering sensitivity

$$\frac{\dot{\psi}}{\delta} = \frac{v_x}{L}$$

i.e. a straight line in figure 7.6-1.

III The understeer vehicle with $K_{us} > 0$ has a maximum which can be calculated by the derivative

$$\frac{d(\dot{\psi} / \delta)}{dv_x} = \frac{L - K_{us} v_x^2}{(L + K_{us} v_x^2)^2}$$

The derivative is zero for

$$v_x^2 = \frac{L}{K_{us}}$$

and this speed is usually called the *characteristic speed*, v_{kar} .

$$v_{kar} = \sqrt{\frac{L}{K_{us}}}$$

Substitution into (7.6.1) gives

$$\left(\frac{\dot{\psi}}{\delta} \right)_{\max} = \frac{v_{kar}}{L + K_{us} \frac{L}{K_{us}}} = \frac{1}{2} \frac{v_{kar}}{L}$$

which is exactly half the steering sensitivity of a neutral steer vehicle at this speed. This fact is sometimes used as the definition of characteristic speed. From the relation between characteristic speed and K_{us}

$$v_{kar}^2 = \frac{L}{K_{us}}$$

it can be seen that this speed decreases the more understeer a vehicle is. Normally, the characteristic speed is in the interval 65 - 100 km/h.

7.7 Evaluation of circular driving tests

Several of the previously mentioned quantities can be determined from circular driving tests. The following equations can be utilized:

$$\delta = \delta_A + K_{us} \cdot a_y \quad (7.7.1)$$

$$a_y = \frac{v_x^2}{R} \quad (7.7.2)$$

$$\delta_A = \frac{L}{R} \quad (7.7.3)$$

$$v_{kar}^2 = \frac{L}{K_{us}} \quad (7.7.4)$$

At a test a vehicle has been driven in a circle with the radius $R = 100$ m. The steering wheel angle and the lateral acceleration at the centre of gravity have been recorded for a number of different speeds. The results are shown in figure 7.7-1.

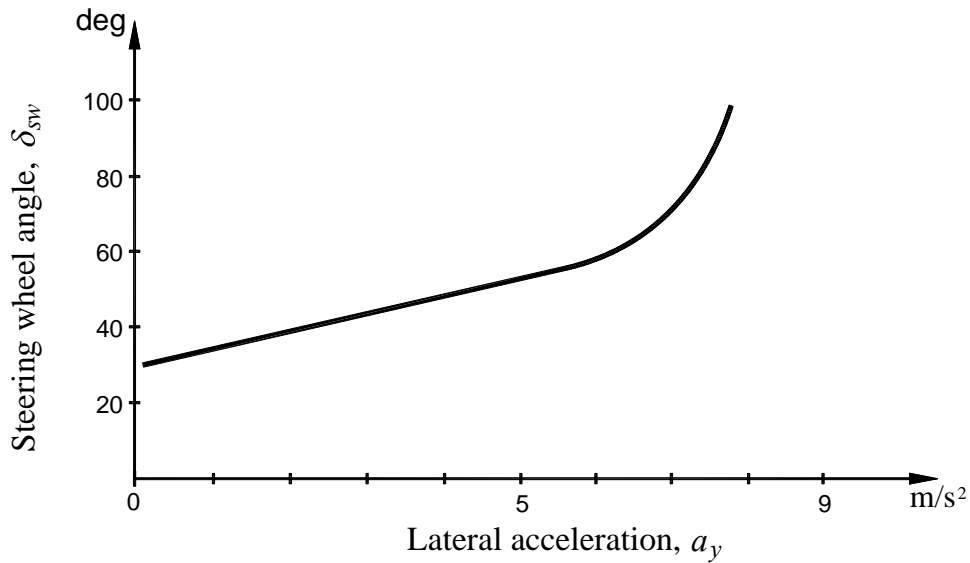


Figure 7.7-1 Lateral acceleration as a function of steering wheel angle.

If the steering ratio is denoted i_s , equation (7.7.1) can be expressed as

$$\delta_{SW} = i_s \cdot \delta = i_s \cdot \delta_A + i_s \cdot K_{us} \cdot a_y$$

In figure 7.7-1, the first term after the last equality sign corresponds to the intersection of the curve with the δ_{SW} -axis, while $i_s \cdot K_{us}$ corresponds to the slope of the curve.

Reading the graph in figure 7.7-1 gives

$$i_s \cdot \delta_A = 30 \cdot \frac{\pi}{180} = \frac{i_s \cdot L}{R}$$

$$i_s \cdot K_{us} = \frac{23}{5} \cdot \frac{\pi}{180}$$

Then

$$v_{kar}^2 = \frac{L}{K_{us}} = \frac{\frac{i_s \cdot L}{i_s \cdot K_{us}}}{R} = \frac{30 \cdot 5}{23} \cdot 100$$

$$v_{kar} = 25,5 \text{ m/s} = 92 \text{ km/h}$$

If the wheel base of the vehicle is known (for example $L = 2.75 \text{ m}$), then K_{us} can be determined as

$$K_{us} = \frac{L}{v_{kar}^2} = 0,00423$$

The steering ration can now be determined since $i_s \cdot K_{us}$ is known from the graph:

$$i_s = \frac{23}{5} \cdot \frac{\pi}{180} \frac{1}{K_{us}} = 19$$

which is a reasonable value.

7.8 Non-stationary driving

In the previous sections, only the stationary case was considered. It was then possible to study differences at steady state circular driving situations. For other kinds of manoeuvres, like slalom driving and entrance and exit from circular driving, it no longer holds that $D \dot{\psi} = D v_y = 0$.

Laplace transformation of equation (7.1.7) yields

$$\begin{array}{ccc} & D \longrightarrow s & \\ \text{Time - domain} & v_y \longrightarrow V_y & \text{Transform - domain} \\ & \dot{\psi} \longrightarrow \dot{\Psi} & \\ & \delta \longrightarrow \Delta & \end{array}$$

$$\begin{pmatrix} A_{11} & A_{12} \\ A_{21} & A_{22} \end{pmatrix} \begin{pmatrix} V_y \\ \dot{\Psi} \end{pmatrix} = \begin{pmatrix} C_1 \\ C_2 \end{pmatrix} \Delta \quad (7.8.1)$$

where

$$\left. \begin{aligned} A_{11} &= m s + \frac{C_{12} + C_{34}}{v_x} \\ A_{12} &= m v_x + \frac{f C_{12} - b C_{34}}{v_x} \\ A_{21} &= \frac{f C_{12} - b C_{34}}{v_x} \\ A_{22} &= J_z s + \frac{f^2 C_{12} + b^2 C_{34}}{v_x} \\ C_1 &= C_{12} \\ C_2 &= f C_{12} \end{aligned} \right\} \quad (7.8.2)$$

Then equation (7.8.1) is

$$\begin{cases} A_{11} V_y + A_{12} \dot{\Psi} = C_1 \Delta \\ A_{21} V_y + A_{22} \dot{\Psi} = C_2 \Delta \end{cases}$$

Solving for $\dot{\Psi}$ and V_y yields

$$V_y = \frac{C_1 A_{22} - C_2 A_{12}}{A_{11} A_{22} - A_{12} A_{21}} \Delta \quad (7.8.3)$$

$$\dot{\psi} = \frac{C_2 A_{11} - C_1 A_{21}}{A_{11} A_{22} - A_{12} A_{21}} \Delta \quad (7.8.4)$$

Substitution of equation (7.8.2) into equation (7.8.3) gives, after simplification

$$\frac{V_y}{\Delta} = \frac{C_{12} J_z s + \frac{b L C_{12} C_{34}}{v_x} - f C_{12} m v_x}{m J_z s^2 + \frac{(f^2 C_{12} + b^2 C_{34}) m + J_z (C_{12} + C_{34})}{v_x} s + \frac{L^2 C_{12} C_{34}}{v_x^2} + m(b C_{34} - f C_{12})} \quad (7.8.5)$$

and

$$\frac{\dot{\psi}}{\Delta} = \frac{f C_{12} m s + \frac{L}{v_x} C_{12} C_{34}}{(\dots\dots\dots)} \quad (7.8.6)$$

This quotient is usually called transfer function, $G_\delta^{\dot{\psi}}$, from the input (the subscript δ) to the output (the superscript $\dot{\psi}$). In this case the transfer function is

$$G_\delta^{\dot{\psi}} = K \frac{1 + T s}{1 + \frac{2\sigma}{\omega_0^2} s + \left(\frac{s}{\omega_0}\right)^2} \quad (7.8.7)$$

where $K = \frac{v_x}{L + K_{us} v_x^2}$

K_{us} = understeer gradient, equation (7.3.7)

$$T = \frac{f m v_x}{L C_{34}}$$

$$\sigma = \frac{m(C_{12} f^2 + C_{34} b^2) + J_z (C_{12} + C_{34})}{2 J_z m v_x}$$

$$\omega_0^2 = \frac{m v_x^2 (C_{34} b - C_{12} f) + C_{12} C_{34} L^2}{J_z m v_x^2} = \frac{C_{12} C_{34} L (K_{us} v_x^2 + L)}{J_z m v_x^2}$$

It is easy to find other transfer functions by combining equations (7.8.5) and (7.8.6) with other simple relations. For example, according to equation (7.1.6) the lateral acceleration is

$$a_y = \dot{v}_y + v_x \dot{\psi}$$

whose Laplace transform is

$$A_y = s G_{\delta}^{v_y} \Delta + v_x G_{\delta}^{\dot{\psi}} \Delta$$

and thus

$$G_{\delta}^{a_y} = \frac{A_y}{\Delta} = s G_{\delta}^{v_y} + v_x G_{\delta}^{\dot{\psi}} = K_1 \frac{1 + \frac{2\sigma'}{(\omega_0')^2} s + \left(\frac{s}{\omega_0'}\right)^2}{1 + \frac{2\sigma}{\omega_0^2} s + \left(\frac{s}{\omega_0}\right)^2} \quad (7.8.8)$$

where

$$K_1 = \frac{v_x^2}{L + K_{us} v_x^2}$$

$$\sigma' = \frac{b}{2 v_x} (\omega_0')^2$$

$$(\omega_0')^2 = \frac{L C_{34}}{J_z}$$

Note that $K_1 = v_x \cdot K$ which corresponds to $a_y = v_x \dot{\psi}$ at circular driving.

For linear dynamical systems of the form in equations (7.8.7) and (7.8.8) there is a rich literature in control theory. Some examples of what is studied are

1. Stability
2. Frequency response
3. Step response

which will be treated in the following sections.

7.9 Stability

The common denominator for the transfer functions in equations (7.8.7) and (7.8.8) is the characteristic equation of the corresponding differential equation. It is well known from mathematics that the roots s_1 and s_2 of the equation

$$s^2 + 2\sigma s + \omega_0^2 = 0$$

are of the form

$$Ae^{s_1 t} + Be^{s_2 t}$$

to the homogeneous differential equation. For bounded solutions when $t \rightarrow \infty$, which implies that disturbances are damped out, a necessary condition is that $\text{Re}(s_1, s_2) < 0$.

In the present special case, the simple vehicle model, $\sigma > 0$. The general solution is

$$s_{1,2} = -\sigma \pm \sqrt{\sigma^2 - \omega_0^2}$$

For an understeer vehicle it follows that $C_{34} \cdot b - C_{12} \cdot f > 0$, which implies that $\omega_0^2 > 0$.

The most common special case is then

I: $\omega_0^2 > \sigma^2 > 0$

Let $\sigma = \zeta \omega_0 \Rightarrow \zeta < 1$

$$s_{1,2} = -\zeta \omega_0 \pm j \omega_0 \sqrt{1 - \zeta^2}$$

where ζ is called the *relative damping*.

The solution corresponds to damped sinusoidal vibrations. It is interesting to observe that in this case

$$\zeta = \frac{\sigma}{\omega_0} = \frac{D_1}{\sqrt{D_2 + D_3 v_x^2}}$$

where $D_{1,2,3}$ are positive constants. The relative damping thus *decreases* with increasing speed.

II: $\sigma^2 \geq \omega_0^2 > 0$

The characteristic equation has a double root or two real roots which correspond to stable solutions.

III $\omega_0^2 < 0$

In this case the solutions are unstable since

$$s_2 = -\sigma + \sqrt{\sigma^2 - \omega_0^2} > 0$$

As previously shown

$$\omega_0^2 = \frac{m v_x^2 (C_{34} b - C_{12} f) + C_{12} C_{34} \cdot L^2}{I_z \cdot m \cdot v_x^2}$$

and it can be concluded that the understeer vehicle for which

$$C_{34} b - C_{12} f < 0$$

is stable when

$$v_x^2 < \frac{C_{12} \cdot C_{34} \cdot L^2}{m(C_{12} \cdot f - C_{34} \cdot b)} = v_{krit}^2$$

and unstable for higher speeds.

7.10 Frequency response properties

It is very common to investigate how the vehicle responds to sinusoidal steering wheel inputs, i.e. of the form

$$\delta = A \sin \omega t$$

The following result from control theory is then very useful.

Def The frequency response function for a linear system refers to the values of the transfer function on the imaginary axis in the complex plane.

The frequency response function $G(j\omega)$ is thus directly obtained by replacing s with $j\omega$ in the corresponding transfer function $G(s)$. The usefulness of this definition, where the real variable ω is interpreted as angular frequency, is clear from the following.

Prop If a linear system with the frequency response function $G(j\omega)$ is exposed to a sinusoidal input $u(t) = A \cdot \sin \omega t$ the corresponding stationary output, under the condition that $G(s)$ only has poles in the left half-plane, will be:

$$Y_s(t) = A \cdot |G(j\omega)| \cdot \sin(\omega t + \angle G(j\omega))$$

where $|G(j\omega)|$ and $\angle G(j\omega)$ denotes the absolute value and the argument of the complex number $G(j\omega)$, respectively, i.e. in polar form $G(j\omega)$ is:

$$G(j\omega) = |G(j\omega)| \cdot e^{j\angle G(j\omega)} = |G(j\omega)| \cdot [\cos \angle G(j\omega) + j \sin \angle G(j\omega)] \quad (7.10.1)$$

If the real and imaginary part of the frequency response function are called $R(\omega)$ and $I(\omega)$, respectively, they can be obtained from equation (7.10.1) as

$$\left. \begin{aligned} R(\omega) &= \operatorname{Re}[G(j\omega)] = |G(j\omega)| \cdot \cos \angle G(j\omega) \\ I(\omega) &= \operatorname{Im}[G(j\omega)] = |G(j\omega)| \cdot \sin \angle G(j\omega) \end{aligned} \right\}$$

and reversely

$$\left. \begin{aligned} |G(j\omega)| &= \sqrt{[R(\omega)]^2 + [I(\omega)]^2} \\ \angle G(j\omega) &= \arctan[I(\omega) / R(\omega)] \end{aligned} \right\}$$

Compare to transformation between polar and rectangular coordinates in figure 7.10-1.

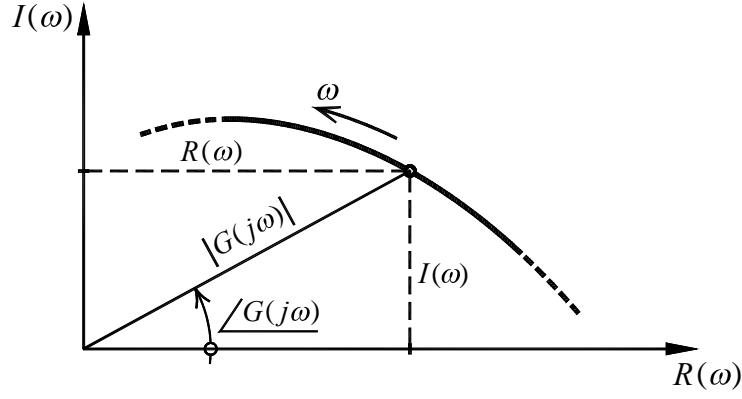


Figure 7.10-1 Different representations in the complex plane.

The polar quantities $|G(j\omega)|$ and $\angle G(j\omega)$ are usually used to represent the frequency response function, rather than the rectangular $R(\omega)$ and $I(\omega)$. The reason is that $|G(j\omega)|$ and $\angle G(j\omega)$ have a direct physical interpretation, namely the change in amplitude and phase a sinusoidal input with angular frequency ω undergoes as it passes through the system. The functions $|G(j\omega)|$ and $\angle G(j\omega)$ (real quantities) are therefore usually called the *amplitude function* and *phase function* of the system, respectively.

In this case, with $s = j\omega$ substituted into equation (7.8.7):

$$G_{\delta}^{\psi}(j\omega) = K \frac{(1 + Tj\omega)\omega_0^2}{-\omega^2 + 2j\zeta\omega_0\omega + \omega_0^2}$$

$$|G_{\delta}^{\psi}| = K \sqrt{\frac{1 + (T\omega)^2}{(\omega_0^2 - \omega^2)^2 + (2\zeta\omega_0\omega)^2}} \cdot \omega_0^2$$

$$\angle G_{\delta}^{\psi} = \arctan(T\omega) - \arctan \frac{2\zeta\omega\omega_0}{\omega_0^2 - \omega^2}$$

Correspondingly, for the lateral acceleration:

$$G_{\delta}^{a_y}(j\omega) = K_1 \frac{1 - (\omega / \omega_0')^2 + 2j\omega(\zeta' / \omega_0')}{1 - (\omega / \omega_0')^2 + 2j\omega(\zeta / \omega_0')}$$

$$|G_{\delta}^{a_y}| = K_1 \sqrt{\frac{(\omega_0'^2 - \omega^2)^2 + (2\zeta'\omega_0'\omega)^2}{(\omega_0 / \omega^2)^2 + (2\zeta\omega_0)^2}} \cdot \left(\frac{\omega_0}{\omega_0'}\right)^2$$

$$\angle G_{\delta}^{a_y} = \arctan \frac{2\zeta'\omega_0'\omega}{\omega_0'^2 - \omega^2} - \arctan \frac{2\zeta\omega_0\omega}{\omega_0^2 - \omega^2}$$

The phase shift $\angle \underline{G}$ can also be expressed as a *time delay* through

$$T(\omega) = \frac{\angle G(j\omega)}{\omega}$$

It could be of interest to investigate how the frequency response properties change for different degrees of understeer, with everything else the same. Frequency response functions for four different parameter combinations, see table 7.10-1, are shown in figure 7.10-2 – 7.10-5. The understeer gradient is varied by changing the front cornering stiffness and the position of the centre of gravity.

Quantity (unit)		Fall 1	Fall 2	Fall 3	Fall 4
m	(kg)	1550	1550	1550	1550
J_z	(kgm ²)	2800	2800	2800	2800
i_s	(-)	17	17	17	17
L	(m)	2,76	2,76	2,65	2,76
f	(m)	1,20	1,33	1,27	1,33
b	(m)	1,56	1,43	1,38	1,43
C_{12}	(kN/rad)	50	71,835	86,032	100
C_{34}	(kN/rad)	150	150	150	150
K_{us}	(rad·s ² /m)	0,01303	0,00620	0,00443	0,00305
v_{kar}	(km/h)	52	76	88	108

Table 7.10-1 Vehicle data used in figures 7.10-2 – 7.10-5.

Examples of field measurements for two real vehicles, corresponding to cases 2 and 3, are also shown in figures 7.10-3 and 7.10-4. It is clear that the simple one-track model shows a reasonable qualitative and quantitative agreement with reality. Results are shown for four different speeds (60, 80, 100 and 120 km/h). Observe that the frequency response functions are plotted with respect to the steering wheel angle $\delta_{sw} = i_s \cdot \delta$ such that:

$$G_{\delta_{sw}}^{\psi} = \frac{1}{i_s} G_{\delta}^{\psi}$$

The comparisons to field measurements should not be taken too seriously. The only known quantities for the vehicles were the understeer gradient K_{us} and the characteristic speed v_{kar} .

It was previously derived that $K_{us} = \frac{m}{L} \frac{(b C_{34} - f C_{12})}{C_{12} \cdot C_{34}}$ and $v_{kar}^2 = \frac{L}{K_{us}}$

The last equation determines L , and by guessing values of C_{34} , f , m , J_z and i_s the curves were plotted.

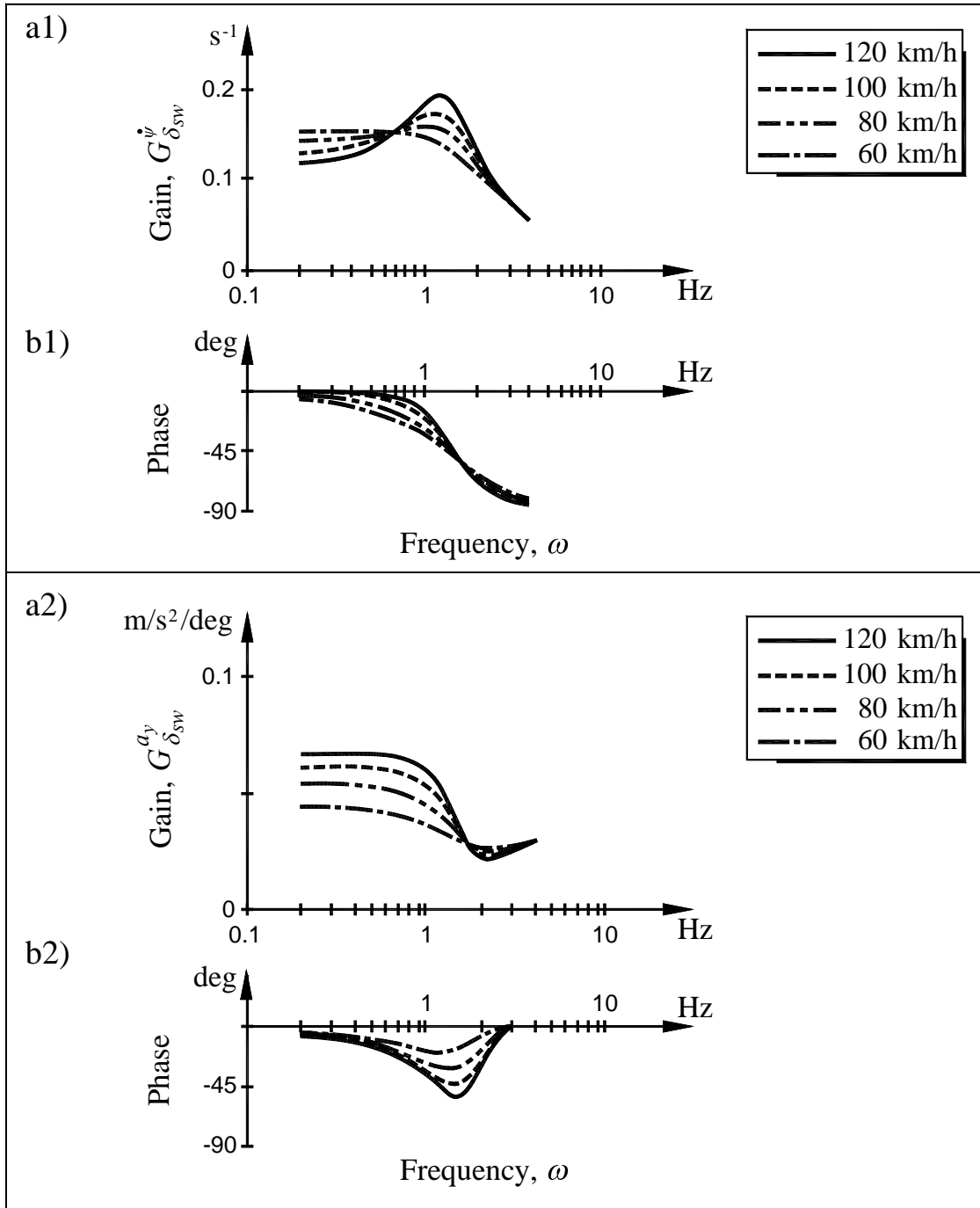


Figure 7.10-2 Gain and phase for the yaw angular velocity and lateral acceleration, divided by steering wheel angle. Vehicle 1 is significantly understeer.

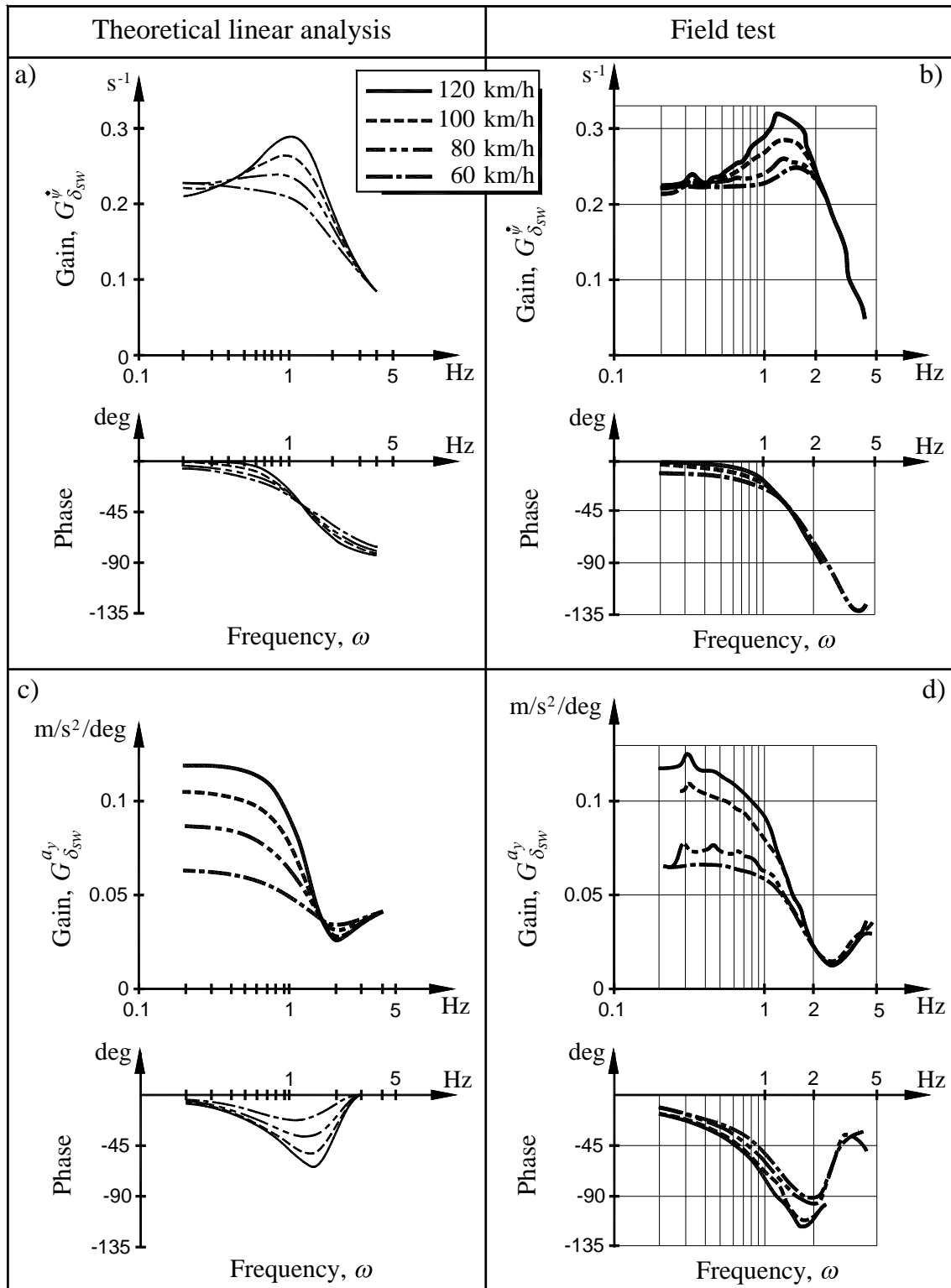


Figure 7.10-3 Gain and phase for the yaw angular velocity and lateral acceleration, divided by steering wheel angle. Vehicle 2 is less understeer than vehicle 1. a) and c) theoretical linear analysis, and b) and d) field measurements.

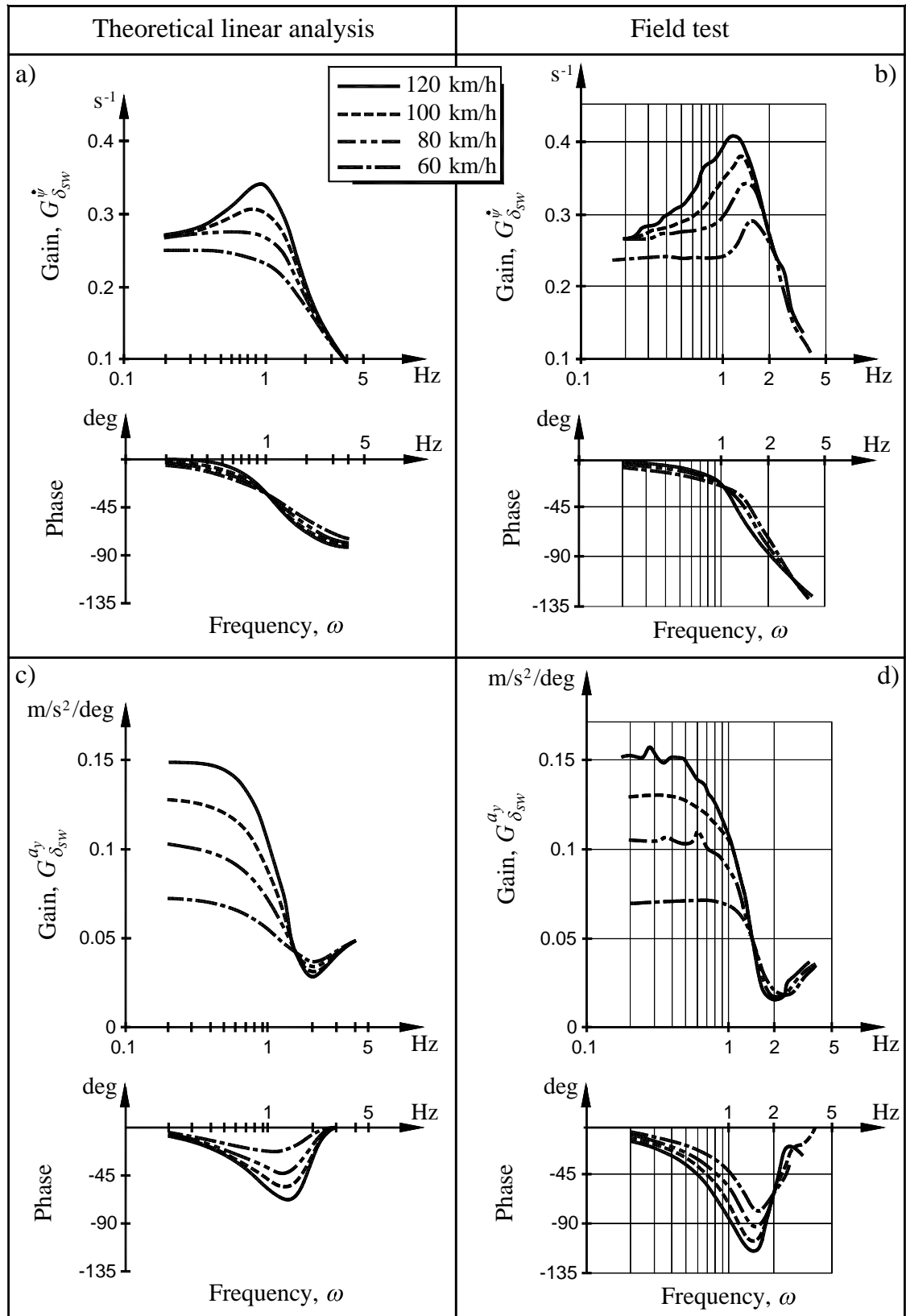


Figure 7.10-4 Gain and phase for the yaw angular velocity and lateral acceleration, divided by steering wheel angle. Vehicle 3 is less understeer than vehicle 2. a) and c) theoretical linear analysis, and b) and d) field measurements.

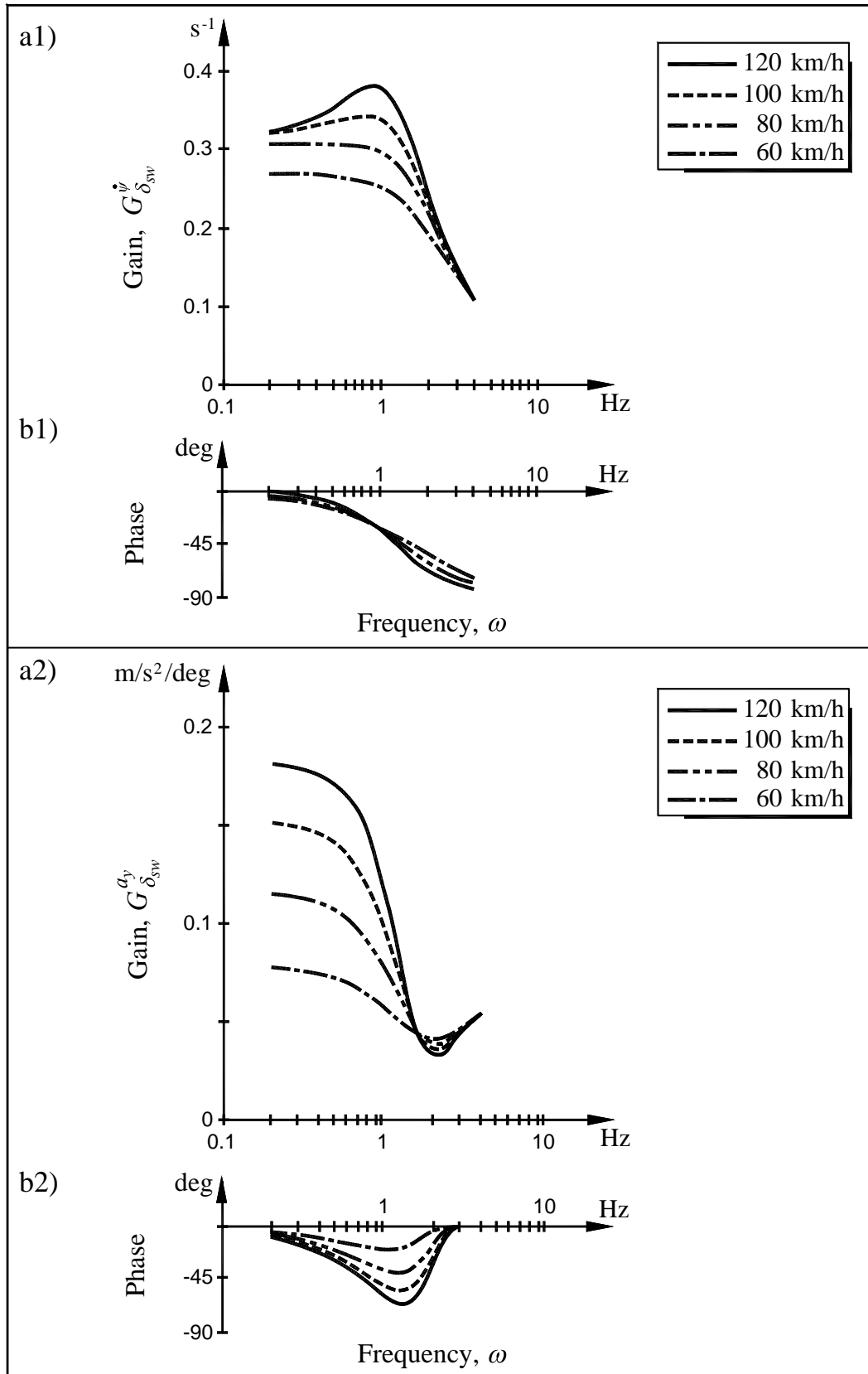


Figure 7.10-5 Gain and phase for the yaw angular velocity and lateral acceleration, divided by steering wheel angle. Vehicle 4, low understeer gradient.

7.11 Step response

Another well known representation of transfer functions is the so called step response, which is easy to calculate with Laplace transforms. The yaw angular velocity is

$$\dot{\Psi} = K \omega_0^2 \frac{1 + T \cdot s}{s^2 + 2\zeta \omega_0 s + \omega_0^2} \Delta$$

If the steering input function is $\delta = \begin{cases} 0 & t < 0 \\ \delta_H & t \geq 0 \end{cases}$

the corresponding Laplace transform is $\Delta = \frac{\delta_H}{s}$

After partial fraction expansion

$$\begin{aligned} \dot{\Psi} &= K \cdot \omega_0^2 \cdot \delta_H \left(\frac{1/\omega_0^2}{s} + \frac{As + B}{s^2 + 2\zeta \omega_0 s + \omega_0^2} \right) = \begin{bmatrix} A = -\frac{1}{\omega_0^2} \\ B = T - \frac{2\zeta}{\omega_0} \end{bmatrix} = \\ &= K \cdot \omega_0^2 \cdot \delta_H \left(\frac{1/\omega_0^2}{s} + \frac{-\frac{s + \zeta \omega_0}{\omega_0^2} - \frac{\zeta}{\omega_0} + T}{(s + \zeta \omega_0)^2 + \omega_0^2(1 - \zeta^2)} \right) \end{aligned}$$

With the adjacent relations between functions in the time and Laplace domain the result, with $\zeta^2 < 1$, is:

$$\dot{\Psi} = K \cdot \delta_H \cdot \left(1 - e^{-\zeta \omega_0 t} \cdot \left(\cos \omega t + \frac{\zeta - \omega_0 T}{\sqrt{1 - \zeta^2}} \sin \omega t \right) \right)$$

where $\omega = \omega_0 \sqrt{1 - \zeta^2}$

$f(t)$	$F(s)$
1	$1/s$
$\sin at$	$\frac{a}{s^2 + a^2}$
$\cos at$	$\frac{s}{s^2 + a^2}$
$e^{at} g(t)$	$G(s-a)$

The corresponding yaw angular velocity response of the four cars in table 7.10-1 is plotted in figures 7.11-1 and 7.11-2.

The first family of curves shows the result for $\delta_H = \frac{1}{i_s} \cdot \delta_{SW}$; $\delta_{SW} = 100^\circ$

The second family of curves is normalized such that the value approaches 1 as $t \rightarrow \infty$. It can be seen that the damping decreases with increasing vehicle speed.

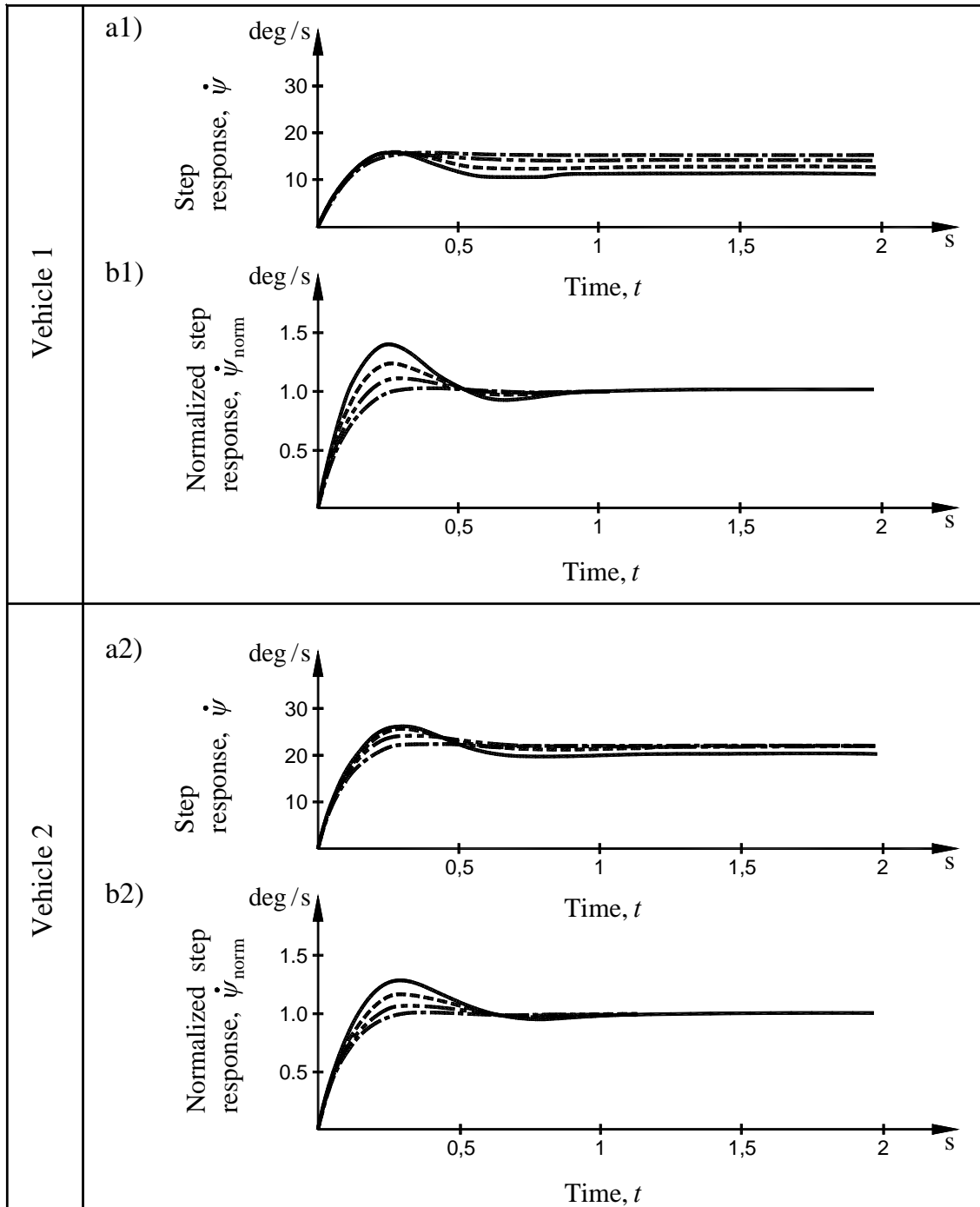


Figure 7.11-1 Yaw angular velocity response for a step function input to the steering wheel. Vehicle 1 and 2 according to table 7.10-1.

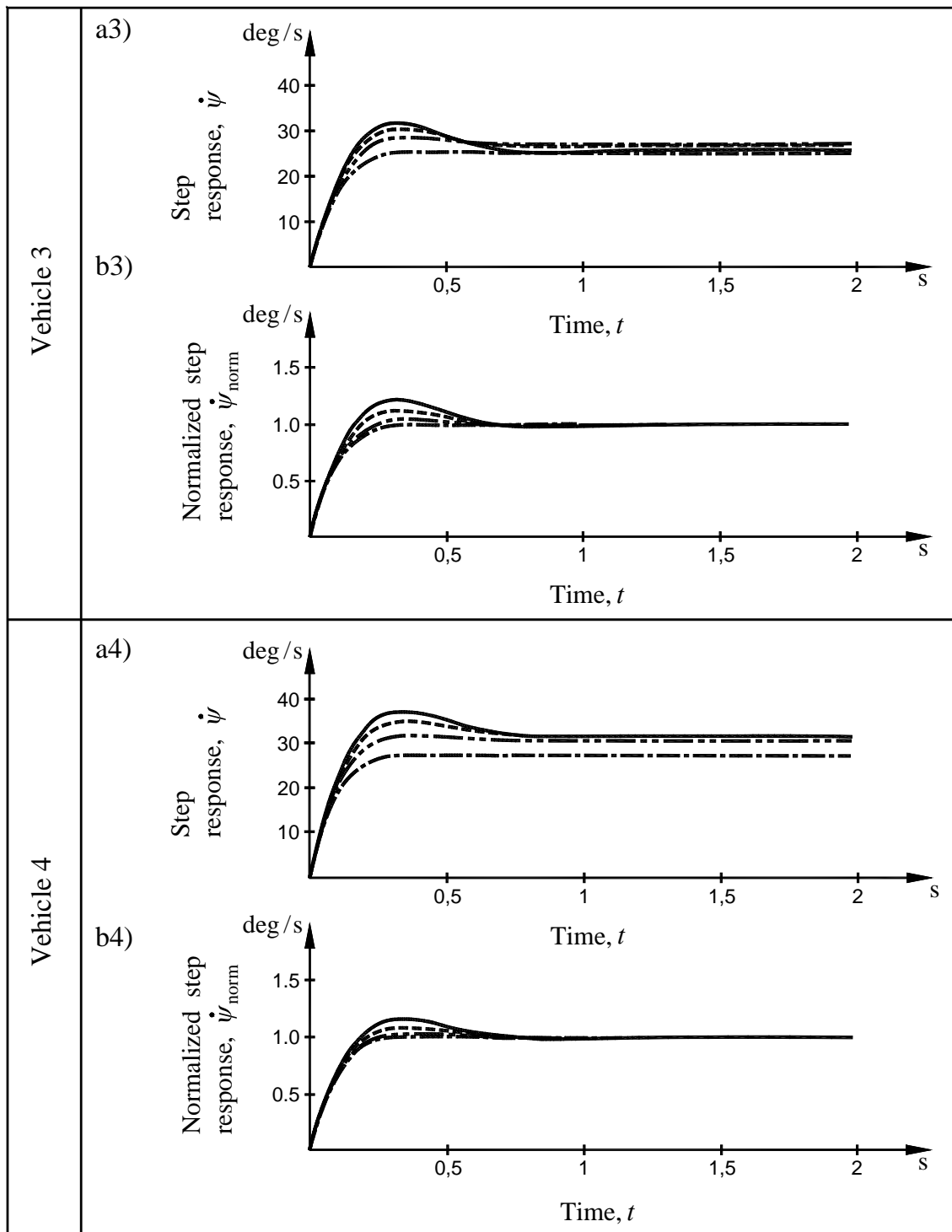


Figure 7.11-2 Yaw angular velocity response for a step function input to the steering wheel. Vehicle 3 and 4 according to table 7.10-1.